Progress In Electromagnetics Research M, Vol. 45, 35–49, 2016

Hybridization of Generalized PO and MoM-GEC Method for Electromagnetic Study of Complex Structures: Application to Reflectarrays

Mohamed Hajji*, Mourad Aidi, Houssemeddine Krraoui, and Taoufik Aguili

Abstract—In this paper, we investigate the diffraction of complex structures applying a new hybridization between generalized PO (Physical Optic) and MoM-GEC method. The proposed approach is developed to speed up convergence, alleviate calculation and then provide a considerable gain in requirements (processing time and memory storage) because it is based on a single test function instead of numerous sinusoidal or polynomial ones. Based on this approach, each metallic pattern is modeled by a current trial function that consists of two parts. The first part is called modal current, and it is decomposed on Hankel functions for modeling metal edges. However, the second part concerns the middle of metallic patterns, and it is modeled by PO method and called generalized PO current. Based on this approach, we study the diffraction of 1D structures, then we generalize our approach to take 2D ones. For validation purpose, we investigate 1D and 2D reflectarrays to prove the new approach's benefits. The obtained results show good accuracy with the method of moments. Moreover, we prove the considerable improvements in CPU time and memory storage achieved by the hybrid approach when studying these structures.

1. INTRODUCTION

The need to enhance microwave and antenna performance is accompanied by a considerable progress in metamaterials research since their discovery. Several structure designs have been proposed in the literature to reach this aim, such as the High Impedance Surfaces (HIS), Reactive Impedance Substrates (RIS), Split Ring Resonators (SRR), reflectarrays and several other structures with different shapes [1–4]. These structures are generally formed by periodic dielectric and metallic patterns with very small periods compared to the wavelength. The use of these particular structures is very interesting since they can provide antenna's miniaturization and high directivity, and optimize performances of microwave circuits. However, they increase the complexity of antennas and microwave circuits because of the important ratio between the smallest and largest dimensions in the same structure. In fact, metamaterial's dimensions are generally very small compared to the wavelength, but the complete structure's dimensions can exceed a few tens of wavelength. This leads to obtaining electric large structures with fine details. The investigation of these complex structures poses a major problem due to the limitation of full wave methods and asymptotic ones. Full wave analysis is often used to model electrically small objects whose dimensions do not exceed a few tens of wavelength, whereas asymptotic methods are used to investigate electrically large objects without fine details. Thus, it is necessary to use multiscale methods [5–9] or the hybridization of numerical methods [10–12] as solutions to overcome the problem of modeling complex structures that contain fine details in large domains. Indeed, the hybridization of numerical methods is one of speediest, efficient and accurate solutions of electromagnetic

Received 22 September 2015, Accepted 11 November 2015, Scheduled 14 December 2015
* Corresponding author: Mohamed Hajji (hadjimed88@yahoo.fr).
The authors are with the Sys'Com Laboratory, National Engineering School of Tunis (ENIT), Tunis El Manar University, B.P.37 Le Belvedere, Tunis 1002, Tunisia.

modeling of complex structures, involving parts with regularly forms and electrical large dimensions, and other smaller parts with complex shapes.

In [13], we have proposed a new hybrid approach joining the MoM method, PO method and a modal approach. It consists in developing a new current test function that can approximate the current distribution on a metallic pattern. Thus, the edges are modeled by infinite cylinders with fine radii and approximated by Hankel functions [14–16]; however, the middle of the metal is governed by PO method. Then, this test function is needed in MoM-GEC process as single to replace a lot of polynomials or sinusoidal ones.

The method of moment combined to the Generalized Equivalent Circuit (MoM-GEC) consists in converting an integral or differential equation into a linear system that will be solved using a matrix representation. The unknown functional is expressed as known functions weighted by unknown coefficients [17–21]. As long as the choice of test functions is consistent, the convergence and physical solution can be rapidly reached. The formulation presented in [13] approximates that metallic patterns are infinite in y direction, so it is applied to 1D structures with invariance in y direction. According to this work, we study the diffraction of 1D periodic structures. Then, we generalize the considered approach to be applied to 2D ones. Hence, we propose to take the current variation in y direction. This is of great interest because it permits the study of bidimensional structures and provides the generalization of our hybrid approach. In this context, for validation purpose, we can investigate the diffraction of 1D and 2D reflectarrays used for antenna's applications. Consequently, we show the advantageous of using our new hybrid approach on different test examples, in terms of accuracy and requirement improvements CPU time and memory storage. In fact, when the number of elements constituting the reflectarrays increases, an enormous gain in CPU time and storage will be achieved.

Otherwise, we choose to validate our approach on reflectarrays due to their interesting advantageous. In fact, reflectarray antennas, as depicted in Figure 1, are mainly formed by printed patches or microstrips over a grounded substrates. The use of this kind of antennas can avoid the problem of their feed network especially at higher frequencies. This can be realized due to their indirect feeding procedure with an external horn antenna. Moreover, reflectarray antennas have many advantageous such as low profile, ease of fabrication, high scanning and tracking capability, and low mechanical complexity. These interesting features permit us to extend the field of applications of reflectarray antennas as in sensing, radar and satellite applications.

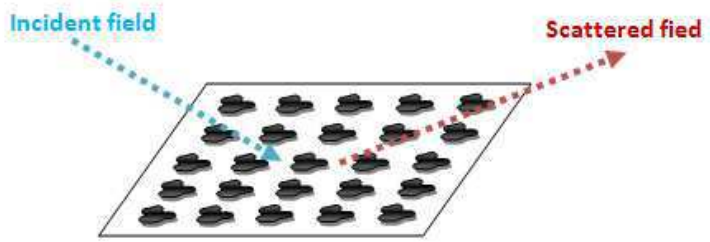

Figure 1. Example of a reflectarray.

The paper is organized as follows. In Section 2, we present the concept of Generalized Equivalent Circuit (GEC) approach used in electromagnetism. Besides, we describe the MoM method combined to the GEC approach. In Section 3, we propose the new hybrid approach and develop the proposed trial function for both 1D and 2D cases. The following section illustrates several test problems of the proposed Hybridization to investigate 1D and 2D reflectarrays. Finally, the improvements in CPU time and memory resources provided by our new approach are demonstrated.

2. DESCRIPTION OF MOM-GEC METHOD

2.1. Principle of Generalized Equivalent Circuit Approach

Electromagnetic phenomenons are always described by Maxwell equations that define the physical laws governing the variation of electric and magnetic fields as a function of time and space. That is why

all numerical methods in electromagnetism are based on the resolution of these equations. In order to reduce the resolution of Maxwell equations, the method of Equivalent Circuits was proposed by Baudrand [18–20] to represent integral equations by Equivalent Circuits. This representation is used to express unknown electromagnetic boundary conditions by only one electric circuit. This electric circuit is considered as an electric form of the studied structure since it describes the discontinuity and its environment. Consequently, the modeling with GEC needs the presence of excitation source, adjustable sources and impedance or admittance operators for illustrating a physical problem.

2.1.1. Excitation Source

The wave exciting the discontinuity surface is represented by a localized or modal source. This source can be a current or field source and is called real source because it can deliver energy. Figures 2(a) and 2(b) depict the representation of real field and current sources [20].

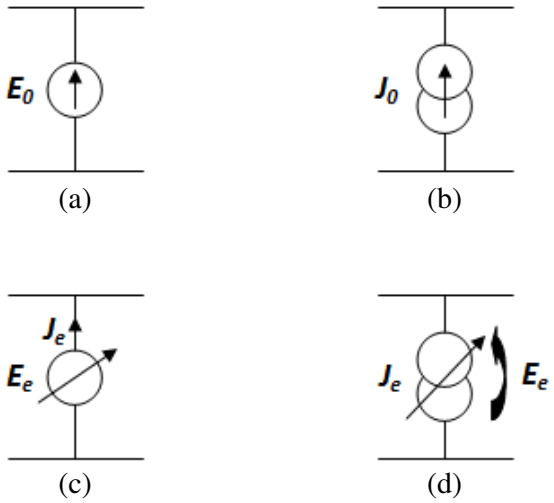

Figure 2. (a) Field excitation source. (b) Current excitation source. (c) Field virtual source. (d) Current virtual source.

2.1.2. Adjustable Sources

The discontinuity is represented by generalized trial functions for describing its electromagnetic state. These trial functions are modeled by virtual sources which do not store energy. The representation by virtual sources permits the expression of all passage relations imposed on electromagnetic field when traversing a discontinuity. We can use the current test function to represent metallic patterns or field test functions to represent dielectric ones. These two representations are shown in Figures 2(c) and 2(d).

The suitable choice of test functions is of great interest to obtain the convergence of the solution, whereas their inadequate choice can complicate the problem or not solve it. Generally, a roughly high number of sinusoidal and triangular test functions is used to get the solution. In this work, we propose a new test function which is only used to replace a lot of sinusoidal or triangular test functions, in order to attain the same results in less time. The proposed trial function is based on physically approximating the current on metal domain in two parts. The first part consists in the current inside the metal. It is governed by PO method. The second one consists in the current on the metal edges. It is modeled by infinite cylinders that provide a diffracted field described by Hankel functions [14–16].

2.1.3. Impedance and Admittance Operators

The discontinuity vicinity is represented by an impedance operator $\hat{Z}$ or an admittance operator $\hat{Y}$ to express the boundary conditions in the two parts of the surface of discontinuity. These operators are

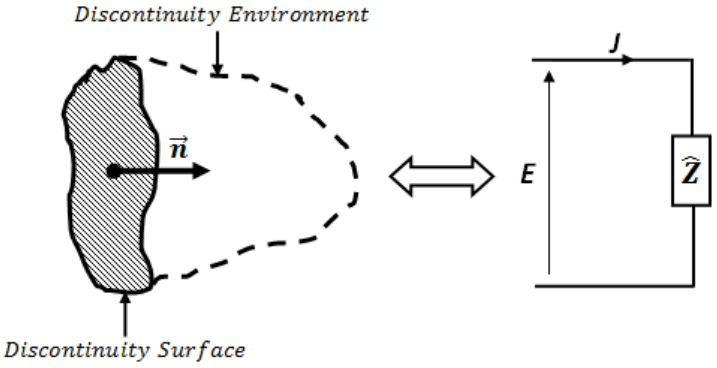

Figure 3. Representation of a discontinuity and its environment by an impedance operator.

used to express the relation between the field and current in this surface by a simple equation. Figure 3 shows the representation of impedance operator.

2.2. MoM Method Combined to the Generalized Equivalent Circuit

The MoM, as all integral methods, permits one to write the boundary conditions in the form of integral equations defined on the studied obstacle's surface. In this way, it leads to reducing the physical problem dimension when it is applied to model planar microwave structures, because it treats tridimensional discontinuities in bidimensional resolution way. This consists of one of the features of integral methods contrary to other numerical methods that need a tridimensional meshing which requires a huge resources. The MoM method is combined to the GEC approach to simplify the modeling of several problems more in electromagnetism.

The modeling of the structures shown in Figure 4, which correspond to different examples of reflectarrays, is done by the GEC given by Figure 5 [13, 17, 18, 21].

Let's surround the refrectarrays formed by N elements with an Electric Magnetic Electric Magnetic (EMEM) waveguide (the horizontal plates of the waveguide correspond to electric boundary conditions however the vertical ones are magnetic ones). We consider $(f_m)_{m\in(1,2,\ldots,M)}$ the modal basis corresponding to the waveguide. E_0 is the excitation modal source that corresponds to the propagative fundamental mode of the waveguide ($E_0 = V_0 f_0$). The impedance operator $\hat{Z}$ describes the environment of the discontinuity. It is used for representing the boundary conditions on its either side and is defined

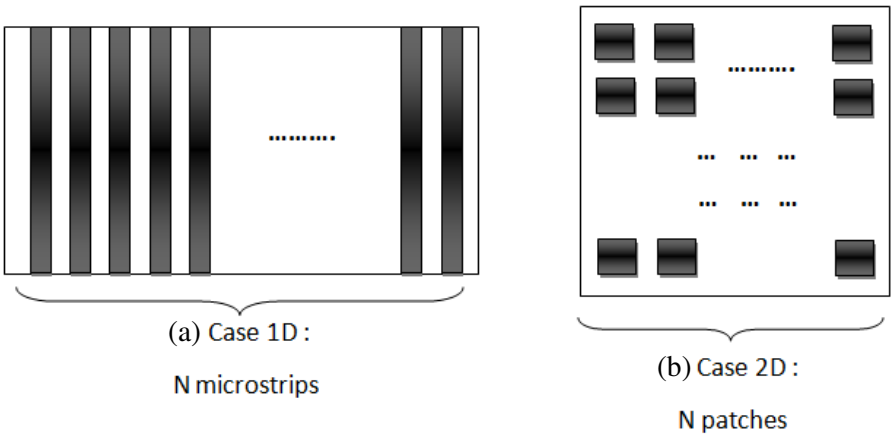

Figure 4. Example of reflectarray. (a) 1D case, (b) 2D case.

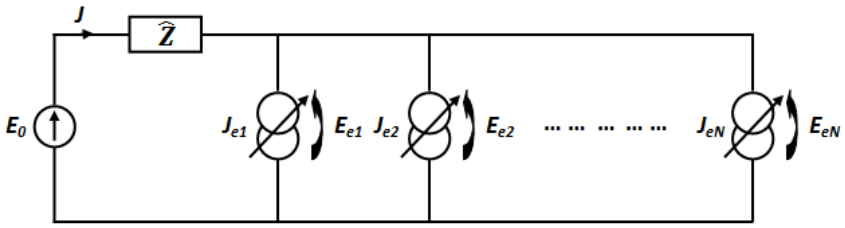

Figure 5. GEC for modeling a reflectarray with N metallic elements.

in function of higher order modes. $(Je)^i_{i\in(1,2,\ldots,N)}$ are the virtual sources defined on the metallic domains of the discontinuity surface. Each test function $(Je)^i_{i\in(1,2,\ldots,N)}$ corresponds to metallic elements in the reflectarray. They are the problem's unknowns expressed as series of known functions $(g_p)^i_{p\in(1,2,\ldots,P)}$ weighted by unknown coefficients $(x_p)^i_{p\in(1,2,\ldots,P)}$.

$$J^i_e = \sum_p x^i_p g^i_p \tag{1}$$

Then, the application of the generalized Ohm and Kirchhoff laws to the GEC shown in Figure 5 leads to obtaining the equations system for $i \in (1, 2, \ldots, N)$:

$$\begin{cases} J = -\sum_{i=1}^{N} J^i_e \\ E^i_e = E_0 - \hat{Z}J = E_0 + \hat{Z}J^1_e + \hat{Z}J^2_e + \ldots + \hat{Z}J^N_e \end{cases} \tag{2}$$

The current J is decomposed on the waveguide basis functions as:

$$J = \sum_m I_m f_m \tag{3}$$

Applying Galerkin's method, we obtain the matrix representation as following [9, 17]

$$\begin{pmatrix} I \\ [0] \\ [0] \\ \cdot \\ \cdot \\ \cdot \\ [0] \end{pmatrix} = \begin{pmatrix} 0 & [-A^T_1] & [-A^T_2] & \cdot & [A^T_p] & \cdot & [-A^T_N] \\ [A_1] & [B_{11}] & [B_{12}] & \cdot & \cdot & \cdot & [B_{1N}] \\ [A_2] & [B_{21}] & \cdot & \cdot & \cdot & \cdot & [B_{2N}] \\ \cdot & \cdot & \cdot & \cdot & \cdot & \cdot\cdot & \cdot \\ [A_i] & \cdot & \cdot & [B_{ij}] & \cdot & \cdot\cdot & \cdot \\ \cdot & \cdot & \cdot & \cdot & \cdot & \cdot\cdot & \cdot \\ [A_N] & [B_{N1}] & \cdot & \cdot & \cdot & \cdot & [B_{NN}] \end{pmatrix} \begin{pmatrix} V_0 \\ [X_1] \\ [X_2] \\ \cdot \\ [X_i] \\ \cdot \\ [X_N] \end{pmatrix} \tag{4}$$

where $[A_i]$ is the excitation vector of the ith metallic pattern; $[A_i] = \langle g^i_p | f_0 \rangle$, $p \in (1 \ldots P)$ (with P is the total used test functions).

However, $[B_{ij}]$ corresponds to the impedance sub-matrix that represents the coupling between the ith and the jth metallic elements, where $(i \in (1 \ldots N),\ j \in (1 \ldots N))$ and $[B_{ij}] = \sum_{mn} \langle g^i_p | f_{mn} \rangle z_{mn} \langle f_{mn} | g^j_q \rangle$. The MoM-GEC consists in describing each metallic element by P test functions, where P is defined by the convergence.

$$[\ A_i\ ] = \begin{pmatrix} \langle g^i_1 | f_0 \rangle \\ \langle g^i_2 | f_0 \rangle \\ \cdot \\ \cdot \\ \cdot \\ \langle g^i_P | f_0 \rangle \end{pmatrix} \tag{5}$$

$$[\ B_{ij}\ ] = \begin{pmatrix} \sum_{mn}\langle g_1^i|f_{mn}\rangle z_{mn}\langle f_{mn}|g_1^j\rangle & \cdot & \cdot & \cdot & \cdot & \sum_{mn}\langle g_1^i|f_{mn}\rangle z_{mn}\langle f_{mn}|g_P^j\rangle \\ \sum_{mn}\langle g_2^i|f_{mn}\rangle z_{mn}\langle f_{mn}|g_1^j\rangle & \cdot & \cdot & \cdot & \cdot & \sum_{mn}\langle g_2^i|f_{mn}\rangle z_{mn}\langle f_{mn}|g_P^j\rangle \\ \cdot & & \cdot & \cdot & \cdot & \cdot \\ \cdot & & \cdot & \cdot & \cdot & \cdot \\ \cdot & & \cdot & \cdot & \cdot & \cdot \\ \sum_{mn}\langle g_P^i|f_{mn}\rangle z_{mn}\langle f_{mn}|g_1^j\rangle & \cdot & \cdot & \cdot & \cdot & \sum_{mn}\langle g_P^i|f_{mn}\rangle z_{mn}\langle f_{mn}|g_P^j\rangle \end{pmatrix} \tag{6}$$

When using P trial functions, each sub excitation vector $[A_i]_{i\in(1\ldots N)}$ is of size (P, 1), and each sub impedance matrix $[B_{ij}]_{(i,j)\in(1\ldots N)}$ is of size (P, P). This leads to obtaining a total excitation vector $[A]$ of size $(N \times P, 1)$ and a matrix $[B]$ with a size ($N \times P$, $N \times P$).

A and B are deduced from the matrix represented by Equation (4) as:

$$[\ A\ ] = \begin{pmatrix} [A_1] \\ [A_2] \\ \cdot \\ \cdot \\ \cdot \\ [A_N] \end{pmatrix} \tag{7}$$

$$[\ B\ ] = \begin{pmatrix} [B_{11}] & [B_{12}] & \cdot & \cdot & \cdot & [B_{1N}] \\ [B_{21}] & \cdot & \cdot & \cdot & \cdot & \cdot \\ \cdot & \cdot & [B_{ij}] & \cdot & \cdot & \cdot \\ \cdot & \cdot & \cdot & \cdot & \cdot & \cdot \\ [B_{N1}] & \cdot & \cdot & \cdot & \cdot & [B_{NN}] \end{pmatrix} \tag{8}$$

The present problem is resolved by the following equations system:

$$\begin{cases} I = -A^T X \\ 0 = AV_0 + BX \end{cases} \tag{9}$$

We can consequently deduce the input impedance of the structure as:

$$Z_{in} = \frac{1}{A^T B^{-1} A} \tag{10}$$

It also permits the determination of weighting coefficients (x_p), current distribution J and diffracted field E_e in the discontinuity surface.

The originality of this work is to propose a new hybrid test function that can be used to replace a lot of sinusoidal or polynomials ones. Hence, P will be equal to 1 ($P = 1$) instead of few tens. This leads to the reducing the sizes of vectors $[A_i]$ and sub-matrices $[B_{ij}]$ to $(1 * 1)$. Consequently, the size of the excitation vector $[A]$ and impedance matrix $[B]$ will be enormously decreased. In fact, we can obtain a total excitation vector $[A]$ of only a size (N, 1) instead of ($N \times P$, 1) and a matrix $[B]$ with only a size (N, N) instead of ($N \times P$, $N \times P$). This hybrid approach is of great interest because it enormously reduces the sizes of manipulated matrices, then an important gain in storage and processing time will be achieved.

3. DEVELOPMENT OF THE HYBRID TEST FUNCTION

3.1. Approximation of Current Test Function for Unidimensional Structures

Let's consider N metallic elements infinite in y direction, in the cross section of a rectangular EMEM waveguides. The structure presents an invariance in y direction. Hence, only TE modes are used to solve this problem. The present problem is similar to a plane wave exciting infinite metallic element. The current test function consists of two parts; the first for modeling metal middle and called Generalized PO current and the second for modeling metal edges and called modal current.

3.1.1. Generalized PO Current

Physical approaches are based on surface current created in the surface of an obstacle illuminated by an electromagnetic wave. The PO method approximates the electric current density $\overrightarrow{J}_{PO}$ on the surface of an object induced by an incident magnetic field $\overrightarrow{H}^{in}$ as [22, 23]:

$$\overrightarrow{J}_{PO} = 2\overrightarrow{H}_{in} \wedge \overrightarrow{z} \tag{11}$$

where $\overrightarrow{H}_{in}$ is the incident magnetic field on the waveguide and $\overrightarrow{z}$ the unit vector normal to the discontinuity that coincides with the propagation direction of the waveguide. $\overrightarrow{H}_{in}$ is deduced from the following equation:

$$\overrightarrow{rot}\overrightarrow{E} = -j\omega\mu_0\overrightarrow{H}_{in} \tag{12}$$

Thus,

$$\overrightarrow{J}_{PO} = \frac{2\beta}{\omega\mu_0}\sqrt{\frac{1}{ab}}\overrightarrow{y} \tag{13}$$

where β is the constant of propagation of the waveguide, μ_0 the air permeability and ω the wave pulsation.

3.1.2. Modal Current

To develop the modal current $\overrightarrow{J}_M$ dependent on x variable, we study the diffraction of a plane wave on fine cylinders with negligible radii modeling the edges. As shown in Figure 6, an incident field E^i, polarized in y direction induces a current in the same direction. The modes excited by the cylinders are decomposed on Hankel functions. Since the cylinder radii are neglected compared to the wavelength, the diffraction phenomenon is governed only by Hankel function of the second kind of order zero [15–17]. Consequently:

$$\overrightarrow{A} = A_0 H_0^2(\beta\rho)\overrightarrow{y} \tag{14}$$

As shown in Figure 6, $R = |\overrightarrow{\rho} - \overrightarrow{\rho'}| = \sqrt{\rho^2 + \rho'^2 - 2\rho\rho'\cos(\phi - \phi')}$, where $\overrightarrow{\rho} = \overrightarrow{OP}$ and $\overrightarrow{\rho'} = \overrightarrow{OM}$ relate the origin O respectively to the observation point P and the source point M.

For the first cylinder, we have $\overrightarrow{\rho} = \overrightarrow{x_1}$, $\overrightarrow{\rho'} = \overrightarrow{x'}$ and $R = |\overrightarrow{\rho} - \overrightarrow{\rho'}| = \sqrt{x_1^2 + x'^2 - 2x_1x'}$.

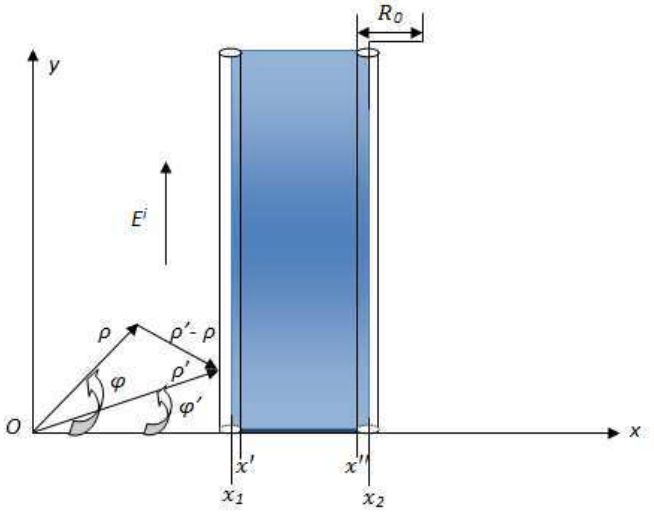

Figure 6. Modeling of current in metal edges by infinite cylinders with fine radii.

The cylinder is assumed infinite, and the observation point P is assumed on the cylinder surface while the source point M is assumed on its axis. Taking into consideration the boundary condition by setting $x' = x_1 + R_0$.

$$E^i + E^d = 0 \tag{15}$$

Thus, the constant A_0 is expressed by:

$$A_0 = \frac{-\sqrt{\frac{1}{ab}}}{j\omega H_0^2(\beta R_0)} \tag{16}$$

Then, the diffracted electric field is expressed as:

$$\begin{cases} \overrightarrow{E}_1^d = \dfrac{-\sqrt{\frac{1}{ab}}}{H_0^2(\beta R_0)} H_0^2(\beta(|x-x'|))\overrightarrow{y}; \quad x' = x_1 + R_0 \\ \overrightarrow{E}_2^d = \dfrac{-\sqrt{\frac{1}{ab}}}{H_0^2(\beta R_0)} H_0^2(\beta(|x-x''|))\overrightarrow{y}; \quad x'' = x_2 - R_0 \end{cases} \tag{17}$$

Consequently, the magnetic field can be deduced as:

$$\begin{cases} \overrightarrow{H}_1^d = \dfrac{\beta}{\mu_0} \dfrac{-\sqrt{\frac{1}{ab}}}{j\omega H_0^2(\beta R_0)} H_1^2(\beta(|x-x'|))\overrightarrow{x}; \quad x' = x_1 + R_0 \\ \overrightarrow{H}_2^d = \dfrac{\beta}{\mu_0} \dfrac{-\sqrt{\frac{1}{ab}}}{j\omega H_0^2(\beta R_0)} H_1^2(\beta(|x-x''|))\overrightarrow{x}; \quad x'' = x_2 - R_0 \end{cases} \tag{18}$$

The modal current is finally concluded by the following expression:

$$\overrightarrow{J}_M = -\left(A_0 \frac{\beta}{\mu_0} H_1^2(\beta|x-x'|) + A_0 \frac{\beta}{\mu_0} H_1^2(\beta|x-x''|) \right) \overrightarrow{y} \tag{19}$$

Finally, the current $\overrightarrow{J}$ dependent on x variable is composed of two parts $\overrightarrow{J}_{PO}$ and $\overrightarrow{J}_M$ ($\overrightarrow{J} = \overrightarrow{J}_{PO} + \overrightarrow{J}_M$), and we will use a single test function dependent on x in MoM-GEC method. Consequently, the test function $\overrightarrow{J}_e$ which will be used in this study to describe the current variation in x direction is expressed as:

$$\overrightarrow{J}_e = -\left(A_0 \frac{\beta}{\mu_0} H_1^2(\beta|x-x'|) + A_0 \frac{\beta}{\mu_0} H_1^2(\beta|x-x''|) + \frac{2\beta}{\omega\mu_0}\sqrt{\frac{1}{ab}} \right) \overrightarrow{y} \tag{20}$$

To avoid the singularity effect of the electric field given by the nature of Hankel functions, the observation point is assumed very close to the edge (cylinder axis), but it remains spaced from it about R_0. Hence, this constitutes the key idea of using the cylinder radius much lower than λ modeling the edges ($R_0 \ll \lambda$).

3.2. Generalization of the Test Function for Bidimensional Structures

Let's consider a metallic patch not infinite in y direction. When it is illuminated by an electromagnetic wave polarized in y direction, an induced current in y direction will be defined on its surface. Because there is no invariance in x nor y direction, since the structure is finite in these directions, the induced current varies as a function of x and y contrary to the case of infinite 1D metallic element when it varies in x direction only.

So, we propose to take into consideration the variation in y direction. Hence, it is known that the incident field in y direction $\overrightarrow{E}_y^{in}$ creates a current density $\overrightarrow{J}_y$ with maximum on its vertical edges and minimum on its horizontal edges.

In this way, we consider that the variation in x direction is carried by the same function as infinite 1D element ($\overrightarrow{J} = \overrightarrow{J}_{PO} + \overrightarrow{J}_{M}$). However, for the dependence in y direction, we propose a sinusoidal variation expressed by $\sin(\frac{q\pi(y-y_i)}{L})$, where y_i corresponds to the minimum horizontal edge's position of the ith patch and $q \in (1 \ldots P)$). Consequently, the generalized hybrid test function for the 2D case is given by the following expression:

$$\overrightarrow{J}_e = -\left(A_0 \frac{\beta}{\mu_0} H_1^2(\beta|x-x'|) + A_0 \frac{\beta}{\mu_0} H_1^2(\beta|x-x''|) + \frac{2\beta}{\omega\mu_0}\sqrt{\frac{1}{ab}}\right) \cdot \sin\left(\frac{q\pi(y-y_i)}{L}\right) \overrightarrow{y} \tag{21}$$

4. APPLICATION OF THE HYBRID APPROACH: STUDY OF REFLECTARRAYS

To validate our approach, we use it to compute the input impedance of reflectarray with N periodic metallic elements. Firstly, we consider the unidimensional case, then we take the case of bidimensional reflectarray formed by N periodic patches. A comparison with MoM-GEC when using sinusoidal test functions is achieved. Moreover, boundary conditions are proved when computing the field and current distributions at the discontinuity surfaces.

4.1. Study of 1D Reflectarrays

We start by studying the diffraction of 1D reflectarray. Thus, we use the hybrid test function to represent the current on each metallic element. Also, we take several cases of the elements number (N) and compute, in each case, the corresponding input impedance.

Figure 7 plots the convergence as a function of the number of used modes of the waveguide for all cases of N. It is noted that the convergence is obtained for about 150 modes for all cases of elements number.

Then, we show the relative error ξ between the input impedance obtained by our hybrid approach and each obtained by MoM method for different considered cases of N (where $\xi = 100 \times \frac{|\|Z_{\text{Hybrid}}\| - \|Z_{\text{MoM}}\||}{\|Z_{\text{MoM}}\|}$).

Figure 8 draws the proposed relative error (ξ) against the number of used elements (N). It is obvious that the error is smaller than 0.5% for all cases. This proves the accuracy of the new method. Another study concerning the domain of validity of the hybrid approach as a function of the fine cylinders radius R_0 is considered for all cases of the number of used elements (N). Indeed, the relative error's (ξ) variation as a function of R_0/λ for different cases of N is shown in Figure 9. For all these cases, the domain $[0.08 * 10^{-3}\lambda - 0.2 * 10^{-3}\lambda]$ corresponds to errors smaller than 1%. Hence, in this domain our proposed hybrid approach is suitable to be applied to study 1D arrays, especially when $R_0 = 0.25 * 10^{-3}\lambda$.

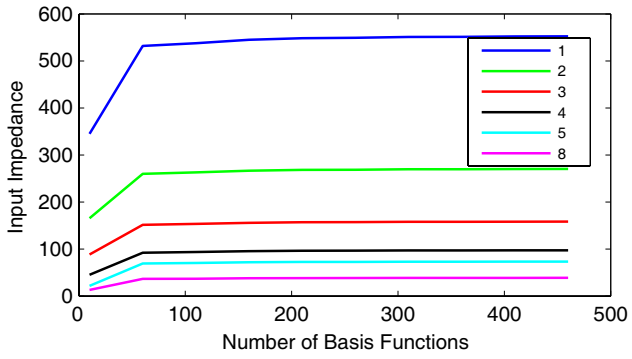

Figure 7. Convergence of input impedance for different number of metallic elements in the 1D case.

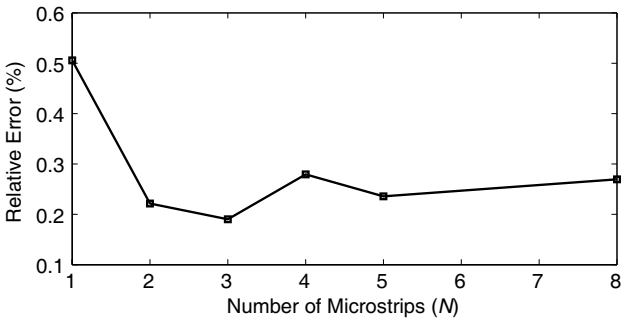

Figure 8. Relative error between the hybrid approach and MoM-GEC (sinusoidal trial functions) to compute the input impedance for different number of 1D metallic elements.

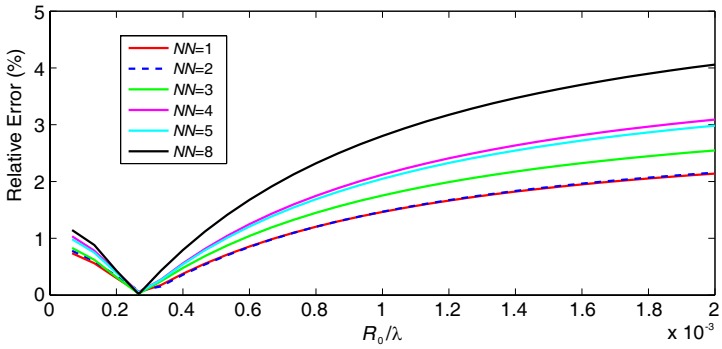

Figure 9. Validity of the Hybrid approach in the 1D case for different number of metallic elements.

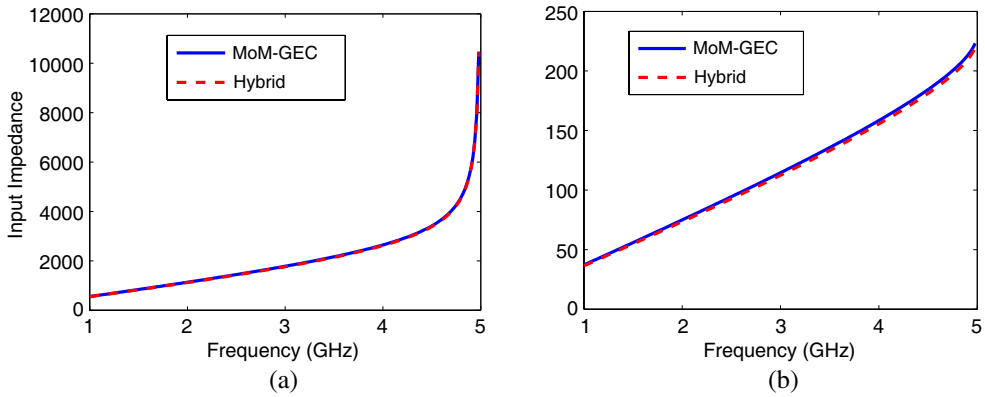

Figure 10. Input impedance obtained by the Hybrid approach for the 1D case at the frequency range [1–5 GHz] and compared to MoM method. (a) $N = 1$, (b) $N = 8$.

Then, the presented approach is validated over a frequency range when $R_0 = 0.25 * 10^{-3}\lambda$. A comparison of the obtained input impedance in the frequency range [1–5 GHz] with MoM method when using sinusoidal test functions is depicted in Figure 10 for two cases of the number of used elements ($N = 1$ and $N = 8$). For the two cases, a good agreement between the two methods at all frequencies is demonstrated.

Besides, we represent the field and current distributions for two cases of number of used elements N ($N = 1$ and $N = 8$) in Figures 11 and 12. Then, a comparison with MoM-GEC when using sinusoidal test functions is achieved. We note a good agreement between obtained results by the two approaches verifying the boundary conditions.

4.2. Study of 2D Reflectarrays

We have generalized the hybrid current test function to be applied to bidimensional structures. In this section, we apply this approach to an example of N reflectarray patches. The patches are in the cross section of an Electric Magnetic Electric Magnetic (EMEM) waveguide.

We investigate the 2D reflectarrays using our hybrid approach and proceed as in 1D case. We start by searching the validity of the hybrid approach as a function of R_0/λ for different numbers of used patches. Figure 13 shows the variation of the relative error between the proposed method and MoM-GEC when varying the number of patches. We note that when the number of used patches increases, the error increases slightly, but it remains smaller than 1% for all cases over the range $[0.6 * 10^{-3}\lambda - 1.5 * 10^{-3}\lambda]$. Consequently, the new hybrid approach is valid to be applied in order to take 2D patch arrays, due to its accuracy especially when $R_0 = 1.1 * 10^{-3}\lambda$. This is of great interest because it provides an enormous improvements of processing time and memory resources.

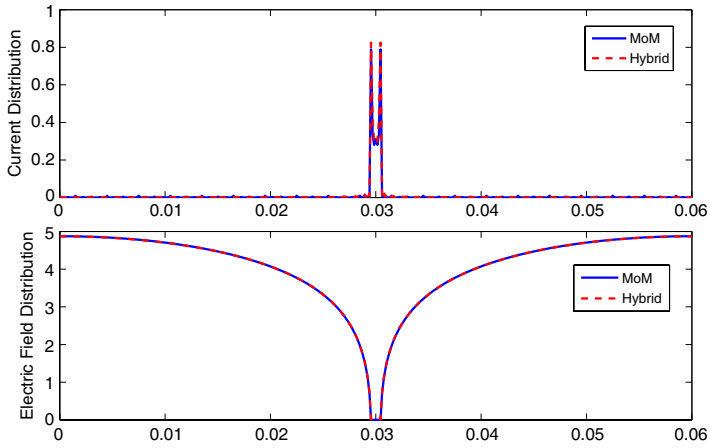

Figure 11. Current and field distributions in the discontinuity surface for one element ($N = 1$). The waveguide length is $A = 60\,\text{mm}$ and the element width is $w = 1\,\text{mm}$ at an operating frequency $F = 1\,\text{GHz}$.

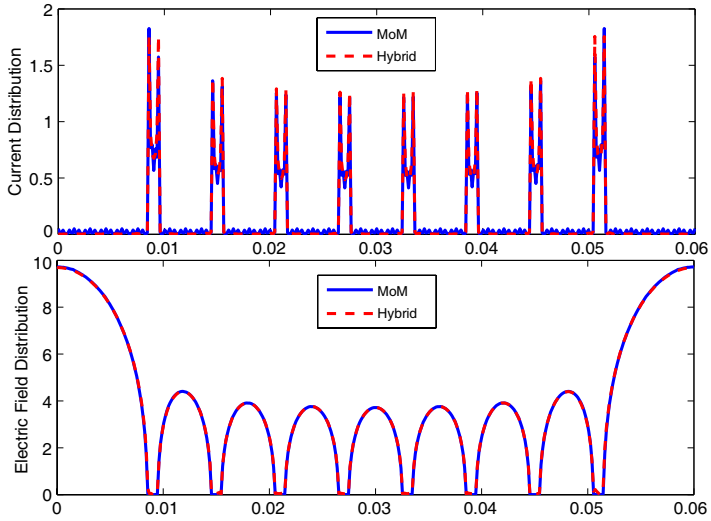

Figure 12. Current and field distributions in the discontinuity surface for eight elements ($N = 8$). The waveguide length is $A = 60\,\text{mm}$, the element width is $w = 1\,\text{mm}$ and the distance between metallic elements is $d = 5\,\text{mm}$ at an operating frequency $F = 1\,\text{GHz}$.

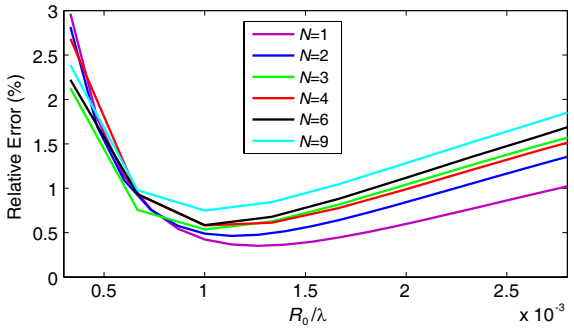

Figure 13. Validity of the Hybrid approach in the 2D case for different number of patches at a frequency $F = 1\,\text{GHz}$.

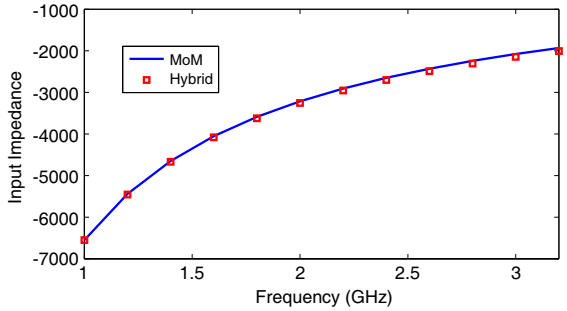

Figure 14. Input impedance obtained by the Hybrid approach at the frequency range [1–3.2 GHz] and compared to MoM method.

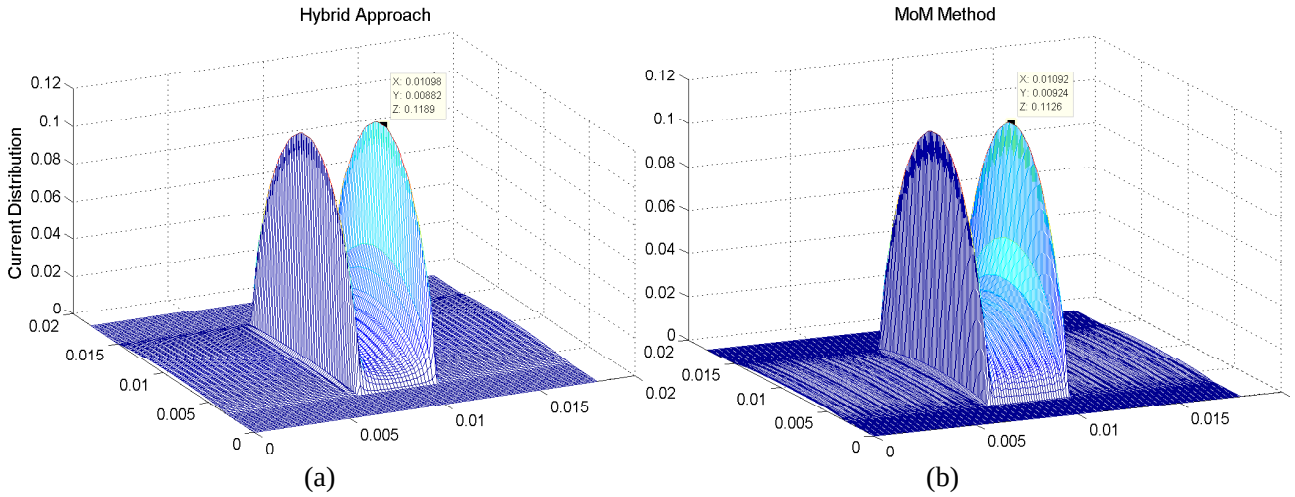

Figure 15. Current distribution on the patch surface at 1 GHz obtained by Hybrid approach and compared to MoM method.

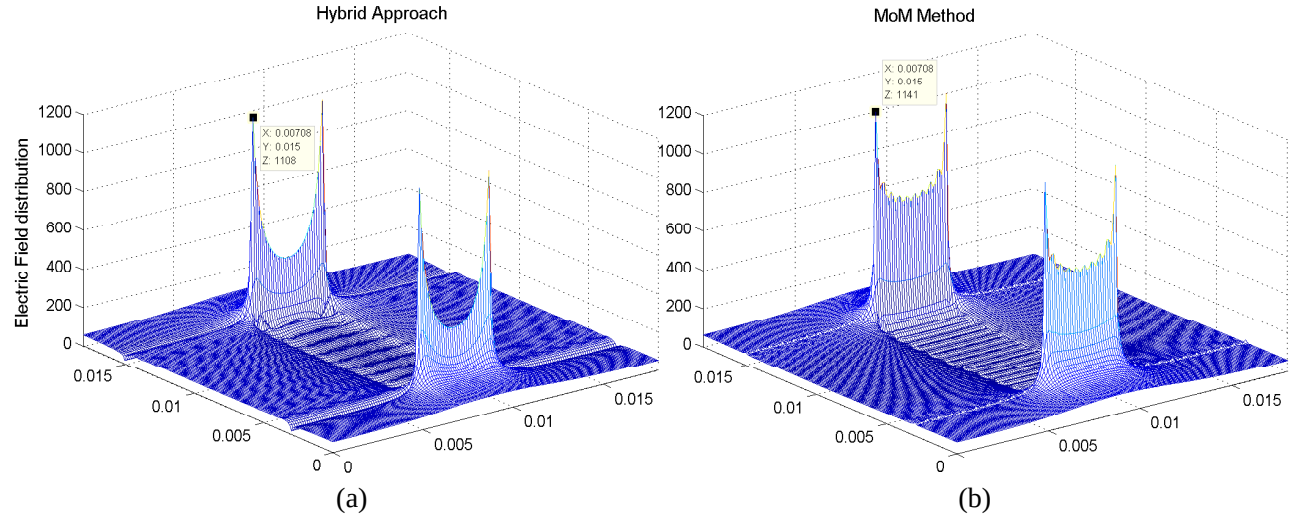

Figure 16. Field distribution on the patch surface at 1 GHz obtained by Hybrid approach and compared to MoM method.

Moreover, similar to 1D case, we validate the hybrid approach over a frequency range. The example treated here is one used patch. So, as shown in Figure 14, this method presents an accuracy over the frequency range [1–3.2 GHz] with an important gain in computational time.

We also verify the boundary conditions for one used patch. Figure 15 shows the current distribution, and Figure 16 shows the field distribution, given by the hybrid approach and compared to MoM method. Consequently, the hybrid approach can be applied to investigate both unidimensional and bidimensional complex structures. It combines the accuracy in results and rapid convergence to alleviate calculation.

5. GAIN IN MEMORY STORAGE AND CPU TIME ACHIEVED BY THE HYBRID APPROACH

The purpose of the hybrid approach proposed in this paper is an important reduction of number of test functions used to attain the convergence. This provides an enormous reduction of the sizes of manipulated matrices. In fact, when computing the input impedance we obtain a reduction in the size of manipulated matrices more than 30 in 1D case and more than 20 in 2D case.

Consequently, this approach permits a considerable gain in memory resources and computational time. To prove these advantages, we evaluate the storage and CPU time provided by the new hybrid approach and compare the obtained results with those of MoM-GEC when using sinusoidal test functions for both of 1D and 2D cases.

5.1. Memory Storage

When using P test functions in each metallic domain (N 1D elements or 2D patches), the MoM method requirements are as:

$$\text{Storage} \propto (N \times P)^2 \tag{22}$$

According to this formula, in the 1D case, when using sinusoidal test functions, we need more than 30 test functions to attain convergence. So, the storage is about $900 * N^2$. On the other hand, when using our hybrid approach, there is a single test function ($P = 1$), so the storage becomes as following:

$$\text{Storage} \propto (N)^2 \tag{23}$$

Consequently, compared to MoM with sinusoidal test functions, a reduction by more than 900 in storage is achieved.

Similarly, in the 2D case, we use $P \times P$ test functions in each patch for MoM with sinusoidal trial functions; however, we use only P test functions in each patch for the hybrid approach. Hence, the storage is $\propto (N \times (P^2))^2$ for the first method and $\propto (N \times (P))^2$ for the hybrid approach. In this way, a gain about P^2 in storage is guaranteed. In major 2D examples, we need about $P = 20$ test functions to reach convergence. So, the gain in storage compared to MoM (sinusoidal trial functions) achieved in the 2D case is about 400.

Figure 17 plots the storage presented by the two methods as a function of metallic elements. An important gain in storage is noted especially when the number of metallic elements increases. This includes the advantage of using this method to treat finite and infinite reflectarrays.

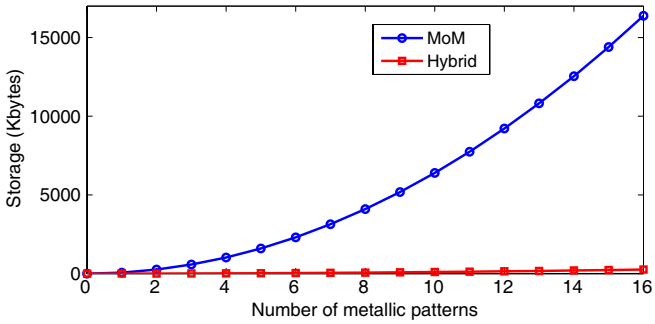

Figure 17. Memory storage required by the Hybrid method compared to each required by MoM-GEC with sinusoidal trial functions against the number of used metallic elements (N).

5.2. CPU Time

To demonstrate the advantageous guaranteed by the new hybrid approach for the two cases 1D and 2D, we plot the CPU time as a function of number of used 1D elements and patches. Figure 18(a) illustrates the 1D case by computing the time needed to calculate the input impedance as a function of 1D elements number. However, Figure 18(b) draws the CPU time used for computing the field and current for the same case.

In the same way, Figure 19 shows the CPU time against the number of patches (2D structure) for the two methods. For both of the cases 1D and 2D, we note the important reduction of time when using the hybrid approach. Moreover, as long as the number of metallic elements increases, a good reduction in CPU time is achieved. Consequently, during this study, we note that the proposed hybrid approach presents a good accuracy for the considered 1D and 2D cases with a considerable improvements in memory resources and CPU time. This allows the presented method to be expected to investigate the diffraction of many complex structures such as reflectarrays.

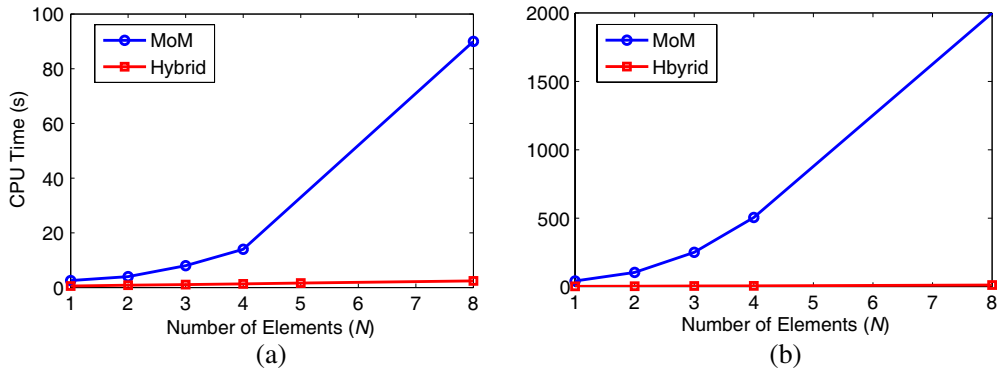

Figure 18. CPU time needed for computing (a) the input impedance and (b) the field and current distributions in the 1D case as a function of number of metallic elements (N).

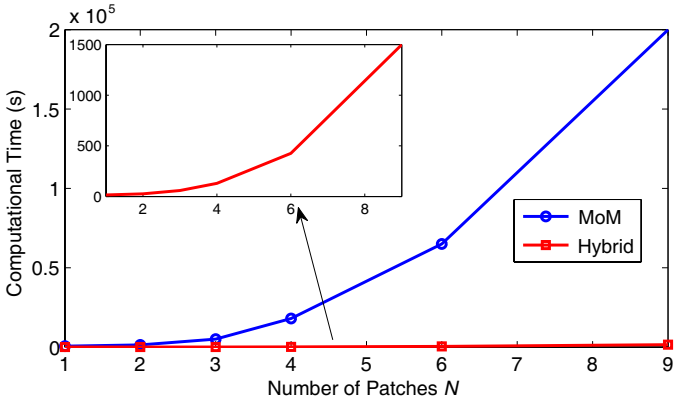

Figure 19. CPU time needed for computing the input impedance in the 2D case as a function of number of patches (N).

6. CONCLUSION

The work presented in this paper concerns a new hybridization between MoM-GEC, modal method and generalized PO. This approach is generalized to take unidimensional and bidimensional complex discontinuities. For validation purpose, we show its accuracy when applied to 1D metallic elements and 2D patches reflectarrays. The major feature of this method is the enormous reduction of sizes of manipulated matrices needed to attain the convergence. This well alleviates the calculation and achieves an enormous gain in CPU time and memory storage especially when the number of metallic patterns in the structure increases.

We have developed the proposed hybridization and shown its accuracy for both 1D and 2D cases of structures. Moreover, we have demonstrated the considerable improvement of the needed requirements when studying these structures.

REFERENCES

1. Sievenpiper, D., "High impedance electromagnetic surfaces," Ph.D. Thesis, UCLA, 1999.
2. Sievenpiper, D., L. Zhang, R. F. Broas, N. G. Alexopoulos, and E. Yablonovitch, "Artificial magnetic conductor surfaces with a forbidden frequency band," *IEEE Trans. Microw. Theory Tech.*, Vol. 47, No. 11, 2059–2074, 1999.
3. Mosallaei, H. and K. Sarabandi, "Antenna miniaturization and bandwidth enhancement using a reactive impedance substrate," *IEEE Trans. Antennas Propag.*, Vol. 52, 2403–2414, Sep. 2004.

4. Sarabandi, K., M. Buerkle Amelia, and H. Mosallaei, "Compact wideband UHF patch antenna on a reactive impedance substrate," *IEEE Antennas and Wireless Propagation Letters*, Vol. 5, 503–506, 2006.
5. Mili, S., C. Larbi Aguili, and T. Aguili, "Study of fractal-shaped structures with PIN diodes using the multi scale method combined to the generalized equivalent circuit modeling," *Progress In Electromagnetics Research B*, Vol. 27, 213–233, 2011.
6. Mili, S. and T. Aguili, "Electromagnetic study of planar pre-fractal structures using the scale changing technique," *2010 18th International Conference IEEE Microwave Radar and Wireless Communications (MIKON)*, Vilnius, Lithuania, 2010.
7. Aubert, H., "The concept of scale-changing network in the global electromagnetic simulation of complex structures," *Progress In Electromagnetics Research B*, Vol. 16, 127–154, 2009.
8. Hajji, M. and T. Aguili, "Contribution of active modes in the formulation of new multi scale approach based on modal operators $\hat{\Gamma}$ and $\hat{Z}_s$," *Conference on Electromagnetic Field Computation: CEFC*, Annecy, May 2014.
9. Hajji, M., B. Hamdi, and T. Aguili, "A new formulation of multiscale method based on modal integral operators," *Journal of Electromagnetic Waves and Applications*, Vol. 29, No. 10, 1257–1280, 2015.
10. Bouche, D. and F. Molinet, *Methodes Asymptotiques en Electromagnetisme [Asymptotic Methods in Electromagnetism], Vol. 16 of Mathematic and Applications*, Springer-Verlag, 1994.
11. Skarlatos, A., R. Schuhmann, and T. Weiland, "Solution of radiation and scattering problems in complex environments using a hybrid finite integration techniques uniform theory of diffraction approach," *IEEE Trans. Antennas and Propagation*, Vol. 53, No. 10, 3347–3575, Oct. 200.
12. Molinet, F., I. Andronov, and D. Bouche, *Asymptotic and Hybrid Methods in Electromagnetics, IET, Vol. 51 of Electromagnetic Waves Series*, 2nd Edition, 2008.
13. Hajji, M., S. Mendil, and T. Aguili, "A new hybrid MoM-GEC asymptotic method for electromagnetic scattering computation in waveguides," *Progress In Electromagnetics Research B*, Vol. 61, 197–210, 2014.
14. Sen, S. G. and M. Kuzuoglu, "Analysis of high frequency plane wave scattering from a double negative cylinder via the modified Watson transformation and Debye expansion," *Progress In Electromagnetics Research*, Vol. 84, 55–92, 2008.
15. Li, C. Y. and D. Lesselier, "On a preliminary analysis of the electromagnetic small-scale modeling of composite panels: Periodic arrangement of circular cylindrical fibers," *Journees Scientifiques URSI-France*, 26–27, Ursi, France, Mar. 2013.
16. Yousif, H. A. and A. Z. Elsherbeni, "Oblique incidence scattering from two eccentric cylinders," *Journal of Electromagnetic Waves and Applications*, Vol. 11, 1273–1288, 1997.
17. Aguili, T., "Modelisation des composants S. H. F planaires par la methode des circuits equivalents generalises," Ph.D. Thesis, National Engineering School of Tunis ENIT, May 2000.
18. Baudrand, H., "Representation by equivalent circuit of the integral methods in microwave passive elements," *IET Microwaves, Antennas and Propagation*, Vol. 2, 1359–1364, Budapest, Hungary, Sep. 10–13, 1990.
19. Aubert, H. and H. Baudrand, *Electromagnetism by Equivalent Circuits*, Editions Cepadues, 2003.
20. Baudrand, H. and D. Bajon, "Equivalent circuit representation for integral formulations of electromagnetic problems," *International Journal of Numerical Modelling-Electronic Networks Devices and Fields*, Vol. 15, 23–57, Jan. 2002.
21. Hajji, M. and T. Aguili, "Studying of surface impedance behavior of RIS against incidence and polarization for miniaturized antenna," *10th International Conference IEEE Loughborough Antennas and Propagation Conference (LAPC)*, 538–542, Loughborough, UK, 2014.
22. Bouche, D. and F. Molinet, *Methodes Asymptotiques en Electromagnetisme, Vol. 16 of Mathematic and Applications*, Springer-Verlag, 1994.
23. Zhao, Y., X.-W. Shi, and L. Xu, "Modeling with NURBS surfaces used for the calculation of RCS," *Progress In Electromagnetic Research*, Vol. 78, 49–59, 2008.